Performance Evaluation of a UWB Vibrotactile Safety Monitoring System for Factory Environments

Sofya Sellak, Oumayma Haberchad, Yassine Salih-Alj
School of Science and Engineering
Al Akhawayn University in Ifrane
Ifrane, Morocco
{S.Sellak, O.Haberchad, Y.Alj}@aui.ma

***Abstract*— This study introduces a safety monitoring system for industry workers. The goal is to monitor the workers' positions in proximity to hazardous zones and deliver timely alerts for potential safety hazards. The proposed system provides tactile proximity alerts by combining vibrating vests with Ultra-Wideband (UWB) position. The suggested system is detailed along with its implementation in a control room. Additionally, the performance of the considered UWB positioning scheme is evaluated, with an emphasis on multipath effects in an industrial environment. The findings provide interesting placement accuracy in both static and dynamic conditions. As a result, it is deduced that the proposed UWB vibrotactile safety monitoring system promises an improved safety for industrial labor with enhanced productivity while lowering the likelihood of accidents and fatalities in such workplace.**

***Index Terms*— Factory Safety; Vibrotactile Guidance; UWB; RTLS.**

I. INTRODUCTION

The industrial sector plays a pivotal role in the growth of economies. In 2022 only, it contributed 28.04 % to the global gross domestic product (GDP) [1]. Most importantly, the sector was responsible for 24 % of total employment in 2022 [2].

However, this increasing need for workers in industrial sites demands for enhancement of safety conditions within indoor factory environments as it remains a paramount priority. For instance, the international labor organization reported an increase in occupational accidents [3]. To make matters worse, around 2.78 million workers die from work related accidents and diseases every year [4]. This demands huge emphasis on worker's safety within factory environments.

To address these concerns, Real-Time Locating Systems (RTLS) have been proposed as an effective solution allowing real-time positioning of workers in multidimensional environments [5]. These systems are based on radio frequency technologies that locate the relative position of the monitored object with respect to devices placed in the instrumented environment.

Given the dense nature of indoor factories, signal fading is a common occurrence for indoor positioning technologies [6]. This requires a selection of communication schemes with high bandwidth, and low fading effects. Ultra-wide band (UWB) wireless communication technology appeared as a suitable solution for indoor factory environments [7]. It allows enhanced positioning accuracy due to its high frequency bandwidth ranging from 500 MHz to 7.5 GHz [8], its strong resistance to interference, low power consumption, and strong penetration ability [9].

Another factor that impacts the safety of workers is safety tools. Traditional methods for communicating hazards relied on auditory alarms and visuals signs. However, such methods are commonly disregarded by workers due to the loud nature of factories [10].

In recent years, haptic signals have been explored as a potential alternative for auditory and visual alarms. These signals allow the perception of transmitted messages through skin receptors [11]. Vibrotactile guiding, in particular, makes use of motors to generate haptic signals with varying duration and intensities providing rapid and precise responses to potential hazards [12].

Proper positioning of vibrating motors heavily affects the performance of the system [13]. Positioning actuators near workers' feet was less effective since little space is available to indicate the location of the hazard. On the other hand, placing them on arms or heads might disturb the workers. In addition to that, different sensations can be emulated depending on the position and the pattern of the vibrators such as calming, guidance, and warning [14].

Limited data availability hinders the evaluations of safety management systems [15]. For instance, data is often collected after incidents occur which makes online monitoring and accident prevention more challenging.

Control rooms have shown promise in providing a more systematic method for automated monitoring and data collection [16], [17]. Introducing them to safety management systems will allow precise evaluation of the positioning scheme used, as well as investigating how workers react to the different messages conveyed by the vibrators.

In this paper, a safety monitoring system based on UWB positioning technology and vibrotactile haptic signals is proposed. The system incorporates vibrating vests alerting workers when entering dangerous zones [18]. A general block diagram of the UWB transmission scheme is further developed

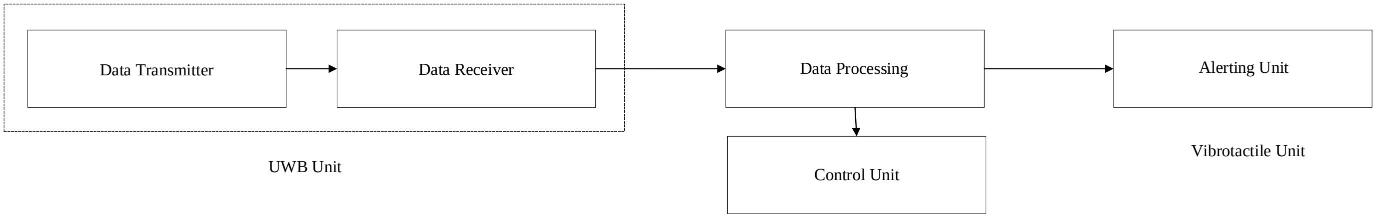

Fig. 1 General block diagram of safety management system.

[19]. Followed by the design of a control room to visualize zones in which the system is implemented, and to collect real-time data. Then, a reinforced analysis on multipath effects in indoor environments is detailed.

This study has the potential to substantially enhance safety awareness in indoor manufacturing sites while improving productivity, which will eventually lead to reduced occupational injuries. Additionally, the system will be a great asset to Morocco by providing safety tools for the industrial sector that is continuously growing with 149 industrial zones currently established [20].

The remainder of this paper is structured as follows. Sec. II details the considered theoretical model for safety monitoring schemes. Sec. III provides a description of the safety management system. Sec. IV presents the simulation results obtained in this study. Sec. V evaluates the performance of the UWB system in an indoor factory environment. Finally, Sec. VI concludes the paper.

II. Theoretical Model of Safety Monitoring System

The general block diagram of the safety monitoring system is illustrated in Fig. 1. Information about the location of the worker is determined using the UWB unit. This information is sent to a processing unit which determines the distance and controls the motors to indicate the presence of hazard [18].

A. UWB Unit

This unit is responsible for locating the workers in danger zones inside the factory using Direct Sequence Ultra-Wideband (DS-UWB) positioning technology. The latter is a wireless technology that allows the transmission of large quantities of data at low powers while resisting multipath degradation effect [21].

B. Processing Unit

Once the location of the worker relative to the danger zones is identified through the UWB unit, the information is sent to the processing unit. The latter consists of microcontrollers with communication protocols that enables the reception and interpretation of the information relayed from the transmitters which will be then used to control the vibrators to alert the worker in the presence of hazard zones.

C. Alerting Unit

The perception of hazard is made possible by the alerting unit. To overcome the limitation of auditory and visual alarms, vibrotactile signals have been selected. Messages indicating the direction of the hazard as well as its intensity are conveyed through vibrating actuators sensed through receptors in the skin.

Vibrating signals have been profiled in [22], based on signal intensity, length, and delay which gave a total of *n* indices. To test these profiles and to identify signals perceived and differentiated by humans, 6,000 random tactile signals have been generated. This allows the calculation of the overlapping area between pairs of signal indices expressed as:

$$A_{ij} = Overlapping\ area\ between\ f_i(x) and\ f_j(x), \quad (1)$$

where $f_i(x)$ and $f_j(x)$ represent the probability density function of the worker's responses to the signal indices *i* and *j* with respect to the signal intensity *x*.

Calculating A_{ij} over *n* indices, proved hat as the index *i* gets closer to index *j*, the overlapping area gets larger, which indicates that the signals are confused by the workers.
To overcome this problem, equation (2) models the groups of signal indices that produce minimal overlapping areas:

$$A(V_r) = min\left(\sum_{i\in V_{r,k}} \sum_{i\in V_{r,k}, i\neq j} A_{ij}\right), \quad (2)$$

for all $k \in \mathbb{N}$ and $2 \leq r \leq n$, with V_r being the set created from combinations of *r* elements from the set of *n* indices, and $V_{r,k}$ the k^{th} element in V_r .

D. Control room

Assessment of the performance of the safety monitoring system is made possible using a control room. The latter refers to centralized units allowing management of complex operations such as transportation systems, production processes, and power generation and distribution [23]. This ensures consistent performance and maintains safety.

The interaction with the system monitored is done using an interface which consists of displays imitating the environment controlled and provides online data varying from videos, equipment status and graphs.

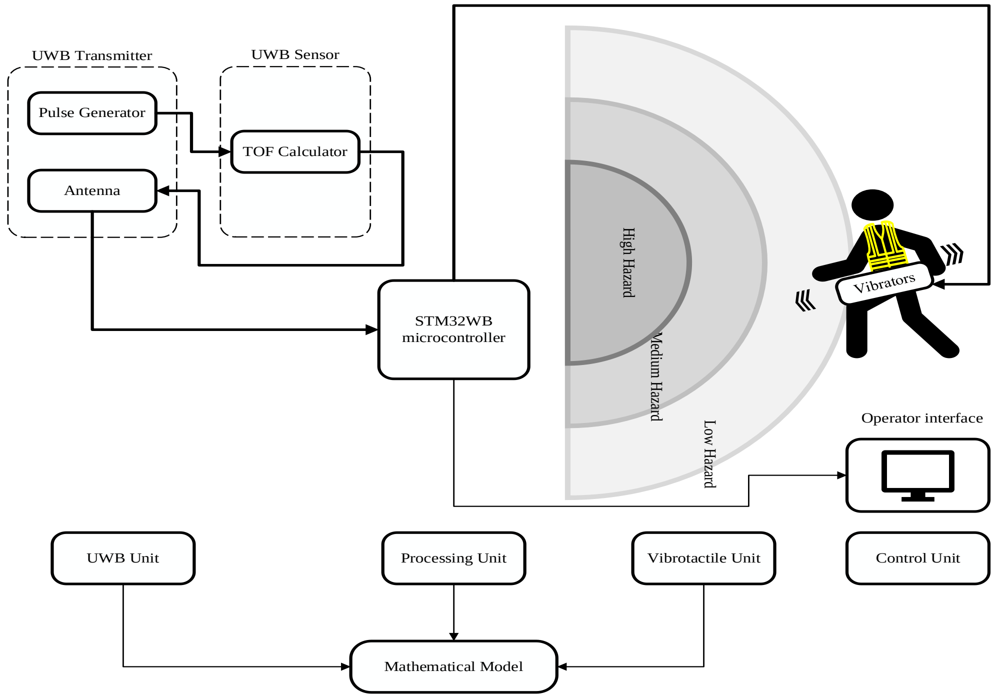

Fig. 2 Diagram detailing the mode of operation of the proposed safety management system.

To design the control room interphase, a set of principles should be followed [24]. First, the information displayed should reflect accurate timing, and proper positioning. Second, the human operator should have the highest authority in the human machine system. Third, a complete and dependable mental model of the system and any related sub-systems should be maintained by the operator. Fourth, operators should acquire pertinent feedback. Fifth, the operator must have access to shortcuts for common control tasks, and complex exchanges should be avoided in favor of straightforward interactions with the system.

III. Suggested Safety Monitoring system for Factory

The suggested safety management system consists of three primary components: a UWB unit for positioning, a processing unit for control, and a vibrotactile unit for alerting, as illustrated in Fig. 2 [19]. The system uses UWB signals for both transmitting and receiving to determine the worker's location within a pre-established danger zone. The details are then transmitted to a processing unit which sends the correct commands to the vibrating actuators of the vibrotactile unit.

A. UWB Unit

1) UWB Transmitter

The DS-UWB signal under consideration consists of small pulses sent across a broad frequency band at a high data rate. The sent data is then extracted by the sensor once it has detected and processed these pulses. The signal that is sent can be expressed as [21]:

$$s(t) = A_{p(t)}p(t)\cos\left(2\pi f_c t + \varphi_{p(t)}\right), \quad (3)$$

where *s(t)* is the transmitted signal, $A_{p(t)}$ is the pulse amplitude, *p(t)* is the pulse shape, f_c is the carrier frequency, and $\varphi_{p(t)}$ is the pulse phase.

The DS-UWB transmitter and sensor are imported from the IEEE 802.15.4z standard MATLAB library. A Decawave DWM1001C module is used as the transmitter. This module has an integrated antenna, a 32-bit ARM Cortex-M0 MCU, and a UWB transceiver featuring a range up to 300 meters.

2) UWB Sensor

To extract the transmitted signal, the received signal is multiplied by a matching filter that has the same impulse response as the pulse originally broadcasted [25]. The output of the matched filter is expressed as follows:

$$r(t) = \int s(\tau) - h(t-\tau)d\tau, \quad (4)$$

where $r(t)$ is the output of the matched filter, $s(\tau)$ is the transmitted signal, $h(t - \tau)$ is the impulse response of the matched filter. The integral is then taken over all possible values of the time-shift τ. After that, the received signal undergoes sampling and quantizing operations to extract the data bits decoded at the receiver.

The Decawave DWM1001-DEV development board is the sensor incorporated into the system. The board consists of a UWB transceiver, a 32-bit ARM Cortex-M0 MCU, and accelerometer and magnetometer sensors.

With the help of the included firmware and software libraries, the DWM1001C module and DWM1001-DEV board can be simply incorporated into STM32-based designs, which makes them compatible with the STM32WB microcontroller.

B. Processing Unit

Two requirements must be met by an adapted microcontroller for the suggested system: Full support of the peripherals required to operate the vibrating motors and a communication scheme tailored for UWB technology. In order to achieve this, the system uses the STM32WB microcontroller, which is capable of supporting UWB communications and includes a number of peripherals, including timers and pulse width modulation (PWM) outputs used to operate vibrating motors. The STM32WB is also highly efficient at preventing multipath fading effects and supports numerous signal routes. Its cost-effectiveness and battery power are two further advantages that make it the ultimate microcontroller for such use.

C. Vibrotactile Unit

A vibrotactile system is adopted as the alerting device for the worker's vest. Four vibrating motors positioned around the waist are linked to an STM32WB microcontroller. This decision is supported by [26], which shows that the waist-belt interface arrangement has better accuracy than the back interface.

Four vibrators are used to indicate the directions: (FL), front right (FR), back left (BL), and back right (BR).On the other hand, Four directions have been emitted (including front (F), back (B), left (L), and right (R)) since it was found in [27], that errors in the perception of direction occur between BR and R, FL and L, FR and R, L and FL, and R and FR.

In addition to that, the hazardous regions considered are predetermined in specific zones in the factory. In Fig. 3, the placement of the actuators and the corresponding direction of hazard is illustrated.

Based on the proximity to the hazardous zones (i.e. low, medium, or high), different vibrating signals with varying intensity, length and delay are generated. Table I details the signal profile of each zone.

In the detailed block diagram depicted in Fig. 4, the process of localization utilizing Ultra-Wideband (UWB) technology is systematically illustrated. Initially, a Gaussian pulse generator is employed to produce ultra-short UWB pulses.

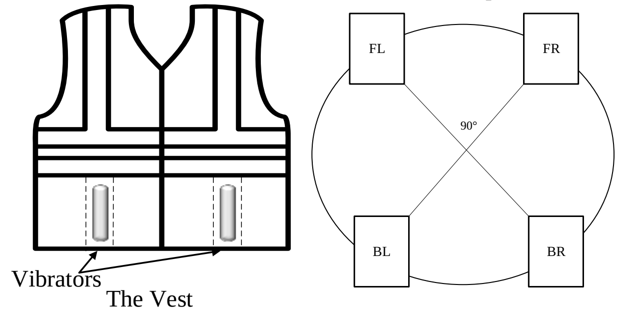

Fig. 3 Diagrams detailing the placement of the vibrators on the workers' vests.

TABLE I.
HAZARD ZONE'S SIGNAL CHARACTERISTICS.

Hazard zone	Number of vibrations	Signal Intensity (V)	Signal length (ms)	Signal delay (ms)
Low	1	1.5	100	100
Medium	2	2.3	300	300
High	3	3.1	500	500

D. UWB Block Diagram

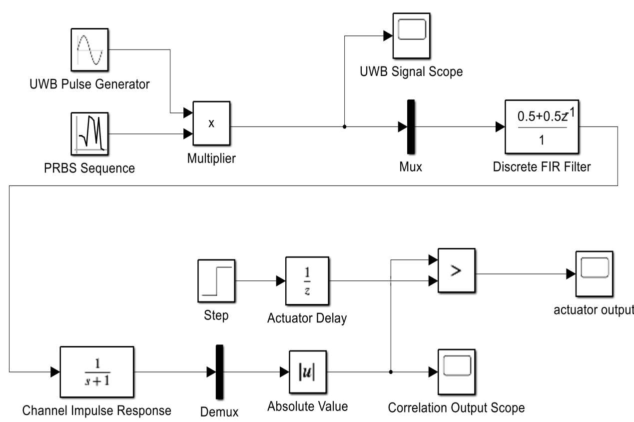

Fig. 4 Block diagram of UWB system using Simulink.

This step is foundational, as these pulses are crucial for achieving high precision in localization efforts. Subsequently, the generated waveforms undergo a process of spreading through the application of a pseudo-random binary sequence (PRBS). This method is instrumental in achieving spectral dispersion, thereby enhancing the signal's resilience against interference, and facilitating improved signal clarity over the transmission range. As the UWB impulses propagate through the designated environment, they are subject to various channel effects. These effects, which can significantly alter the signal propagation and reception, are encapsulated within a modelled impulse response of the channel. This modeling is crucial for accurately representing the channel's impact on the signal and for developing strategies to mitigate adverse effects, ensuring signal integrity is maintained.

Upon arrival at the targeted location, the UWB signal is intercepted by a designated sensor, tasked with capturing the signal. The captured signal is then analyzed through correlation with the PRBS to verify the presence of a moving object, such as a person. This verification process involves applying a threshold to the correlation output, a critical step that ensures the detection mechanism's reliability and accuracy.

In instances where motion is detected, the system triggers a sequence of actions leading to the activation of a vest's vibrating mechanism, which subsequently results in the emission of a vibrating alarm. This operational sequence is integral to the system's design for alerting the presence of motion. The block diagram serves as a vital tool for simulating and evaluating the system's performance, particularly focusing on aspects such as detection accuracy and the response time of the vibration actuators to detected motion.

Fig. 5 illustrates the synthesis of a UWB signal by combining a predetermined pulse shape with the PRBS. This synthesis yields a signal characterized by a 1 ns pulse duration and a 1 V amplitude, generated at a sampling frequency of 10 GHz. This diagram is essential for elucidating the transmitted signal's properties and its interaction with the PRBS sequence, thereby providing insights into the signal's behavior and its propagation characteristics.

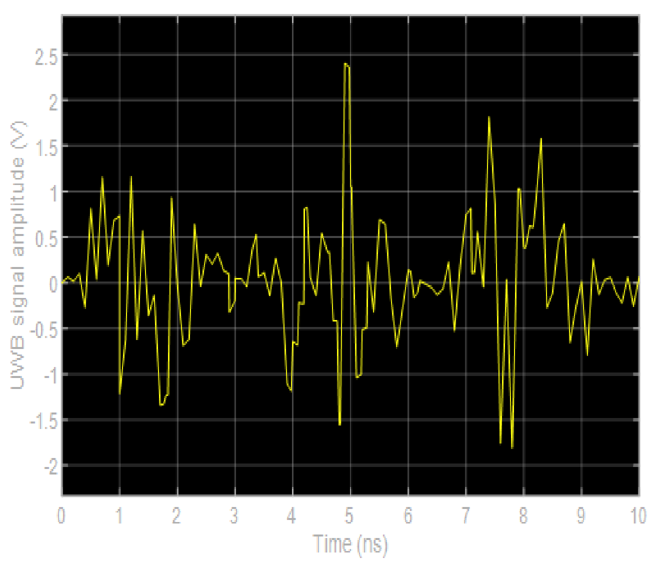

Fig. 5 UWB Signal.

The correlation output scope graph, presented in Fig. 6, is instrumental for monitoring the detection of motion or the presence of an individual near the sensor in real-time. It displays the correlation output between the received UWB signal and the PRBS sequence, highlighting significant correlation levels that indicate motion detection. The observed spikes in the correlation output signal the moments of strong alignment between the received signal and the PRBS sequence, denoting the detection of movement.

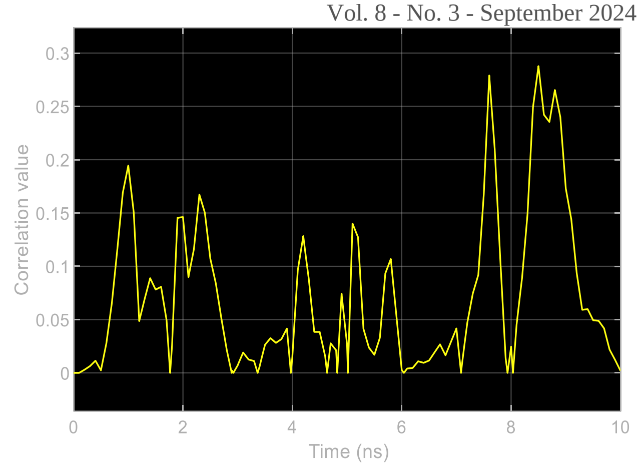

Fig. 6 Illustration of a correlation signal.

Additionally, in Fig. 7, the actuator output scope graph sheds light on the timing and delay associated with the activation of the vibration actuator following motion detection. This graph illustrates the actuator's response delay, quantified as 0.1 s, transitioning from a state of inactivity to activation, depicted as a step signal. This visualization is pivotal for assessing the actuator's response timing and delay in reaction to motion detection, offering valuable insights into the system's operational effectiveness.

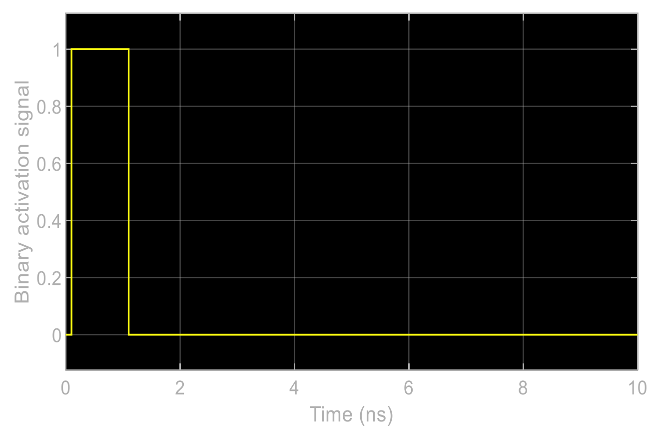

Fig. 7 Considered step response for the actuator's output.

E. Control Room Interface

The suggested safety monitoring system, illustrated in Figs. 8 and 9, is designed to incorporate an interface that visualizes the factory's environment where it is deployed, focusing particularly on the dangerous areas marked by UWB blocks. Information from the microcontroller attached to each vest is shown in the control room, detailing how far the workers are from these hazardous zones, along with the feedback from the vibrators. This setup facilitates the assessment of the system's effectiveness in two main areas: the vibrators' reaction to the proximity of danger zones and how workers engage with this mechanism.

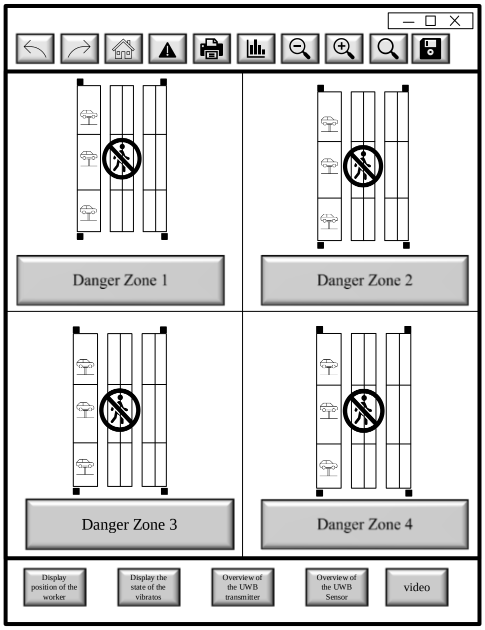

Fig. 8 Overview of the developed user interface for the control room.

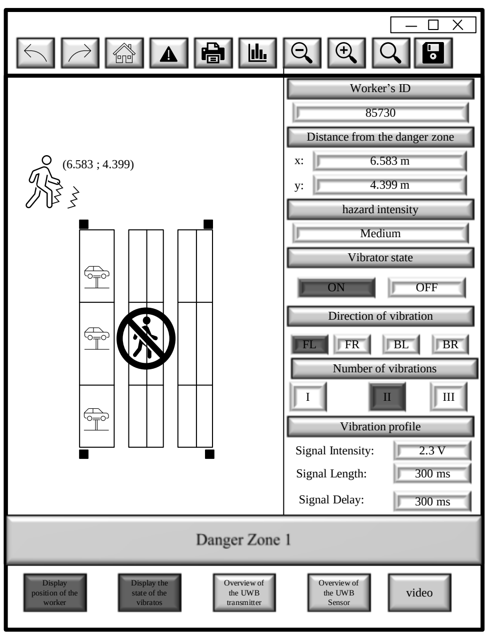

Fig. 9 Display of worker's position and state of vibrators in user interface.

IV. SIMULATION RESULTS

In a hazardous environment, a communication system employing stationary Ultra-Wideband (UWB) transmitters and sensors has been deployed to bolster workers safety. The system operates by issuing a vibratory alert to a worker's jacket when any movement is identified within the range of a UWB unit. This capability for passive movement detection is enabled through simulations based on the IEEE 802.15.4z standard, which is instrumental in averting potential dangers in such environments.

The functionality of the IEEE 802.15.4z standard for UWB communication in the accurate estimation of a device's location is demonstrated through a simulation utilizing the one-way ranging/time-difference of arrival (OWR/TDOA) method.

In this setup, a worker's transceiver emits short signals, known as "blinks", which are captured by a set of synchronized infrastructure nodes which represent the UWB unit, designated as A, B, C, and D. These nodes, which double as stationary UWB transmitters/sensors, are positioned at specified coordinates, with node A at $x = 40$, $y = 41$; node B at $x = 62$, $y = 83$; node C at $x = 87$, $y = 24$; and node D at $x = 10$, $y = 80$. The distribution of these signals and the process of locating the worker are depicted through illustrative figures (Figs. 10 and 11). The worker's position is determined by the intersection of hyperbolic surfaces generated from the TDOA between the periodic signals from each pair of synchronized nodes, achieving a localization precision within 6 centimeters. This precision is assessed through the Euclidean distance among the intersecting points of the hyperbolic surfaces and the actual location of the worker.

The aim within the scope of UWB localization technology is to ascertain the location of a worker equipped with a vest, using TDOA estimates for localization upon receiving the signal from the UWB module. When the worker comes within the range of the related unit, the latter signals the microcontroller, which, in turn, activates a vibration motor, providing haptic alert to the worker in the direction of the hazard.

The performance of this UWB localization system has been evaluated under both static and dynamic conditions, reporting a median localization error of less than 12 centimeters for static conditions and less than 28 centimeters for dynamic conditions, as indicated in the literature [28]. This demonstrates the system's effectiveness and accuracy in enhancing worker safety in hazardous environments.

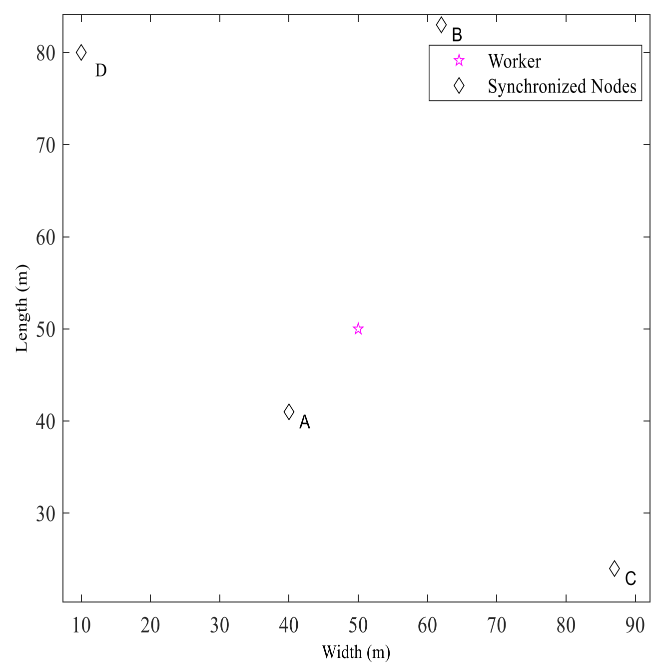

Fig. 10 Network setup for synchronized nodes and device in 100 x 100 plane: location visualization.

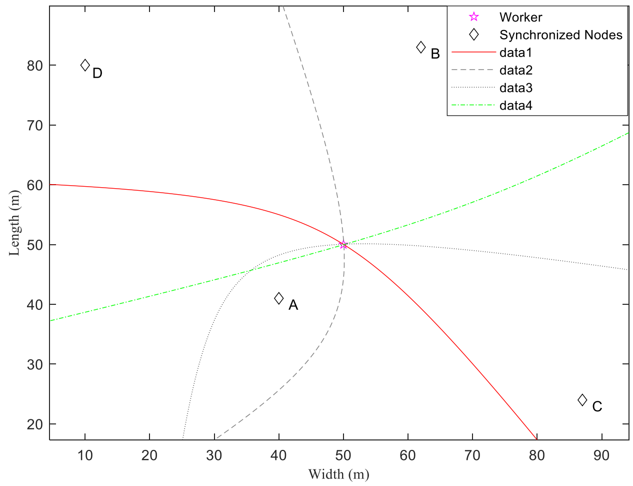

Fig. 11 Intersection of hyperbolic surfaces for device position estimation: 2D curve plot analysis.

V. Performance Evaluation of the UWB Positioning System

The performance of the proposed system, specifically in terms of UWB positioning in indoor manufacturing environments, has been evaluated. Examining the performance of UWB signals in specific environmental conditions was carried out using MATLAB's IEEE 802.15.4a UWB channel modeling tools [29]. This modeling is crucial for the development of systems that are capable of effectively handling the complex signal dynamics found in indoor environments.

At first, the channel was defined for use in an industrial environment, considering a line-of-sight (LOS) factor. The industrial environment was characterized by setting parameters including path loss exponent, shadowing deviation, and antenna loss. Afterwards, a sent signal was set at a specific power level, and calculations for path loss were conducted, considering the distance and frequency characteristics typical of the industrial setting.

Clusterization was then performed, grouping path gains into separate clusters. This technique replicated the reflections and diffractions encountered by UWB signals in an industrial environment, crucial for understanding the time delay and multipath effects that may influence positioning accuracy. Next, path modeling continued by assigning arrival times, average powers, and phases to the multipath components. Small-scale fading was implemented by adjusting Nakagami distribution parameters to introduce fluctuations in signal amplitude, which were affected by the complexities of the industrial environment.

The simulations were made easier with the use of algorithms such as the adjusted Saleh-Valenzuela model for representing multipath elements in separate groups and the Nakagami distribution for small-scale signal variations. The first one was selected for its effectiveness in simulating the grouped arrival of multipath components, while the second one is known for its flexibility in depicting various fading conditions seen in wireless channels.

During the simulation, these algorithms were tested on various channel scenarios representing different environmental movements, determined by factors such as sample density and Doppler shift. The result of these procedures was a set of path gains that captured how the signal changed because of the channel's multipath features.

Fig. 12 shows the UWB channel in an indoor industrial setting, which is defined by three separate clusters. Cluster 1, shown in yellow, demonstrates path gains beginning at about 0.12 and decreasing to approximately 60 ns. Cluster 2 is highlighted in red and ranges from slightly above 0.10 to around 80 ns. Ultimately, the blue Cluster 3 commences around 0.08 and fades after 100 ns. The range of path gains in each cluster shows the diversity caused by multipath effects and small-scale fading in the arrival time of the signal.

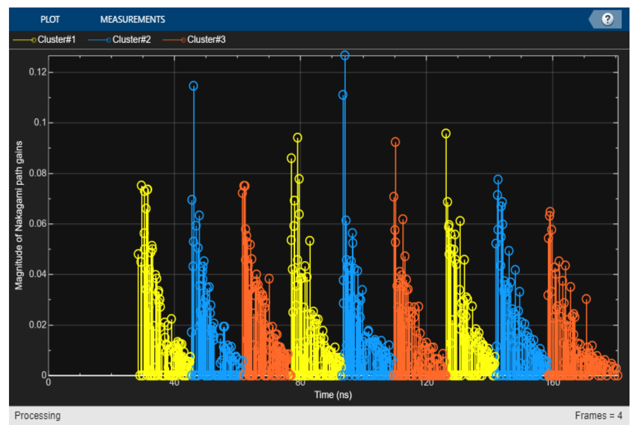

Fig. 12 Indoor industrial environment Nakagami path gains plot.

In Fig. 13, the scatter plot in the indoor industrial setting, before using the channel model, displays ternary symbols anticipated at -4, 0, and +4 on the in-phase axis. This signifies a clean beginning signal, showing an undistorted transmitted signal where symbols do not deviate much from three distinct levels.

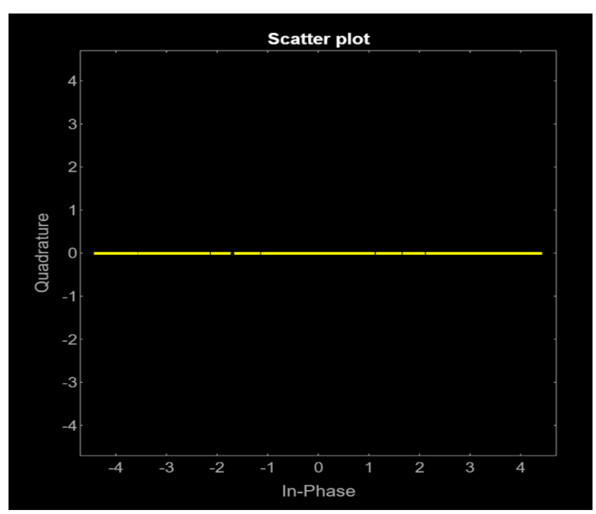

Fig. 13 Industrial environment UWB transmitted signal scatter plot before channel effects.

Fig. 14 shows the scatter plot of the signal following its passage through the simulated industrial channel. The points create a crowded cluster, where the values are predominantly between -1.5 x 10-4 and +1.5 x 10-4 in phase, with quadrature components reaching similar values. The distribution of points shows how the channel affects signal dispersion and introduces significant noise from multipath fading and inter-symbol interference.

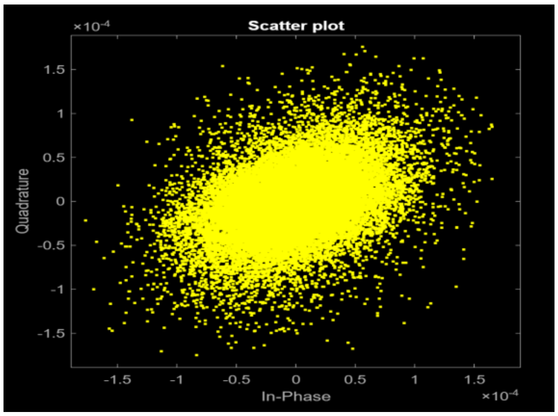

Fig. 14 Industrial environment UWB signal scatter plot after channel effects.

Fig. 15 illustrates a unique channel characteristic commonly seen in outdoor settings. In this visual, one dominant group is shown, with path gains reaching slightly over 0.14. The paths arrive within about 100 ns, indicating a less crowded environment or a dominant direct line-of-sight with fewer reflections.

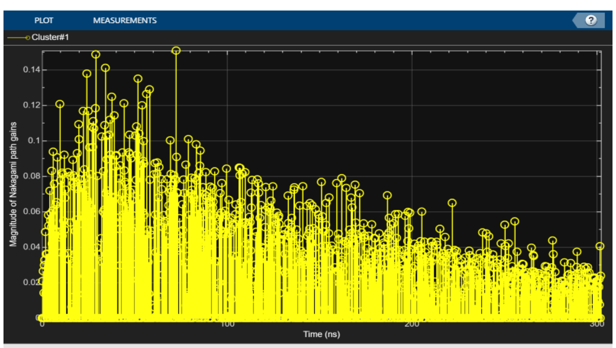

Fig. 15 Outdoor environment Nakagami path gains plot.

Fig. 16 shows a comparison of UWB channels in outdoor and industrial settings. Multiple clusters are identified as Cluster 1 to Cluster 14, each having different path gains and arrival times. The clusters show considerable time spread with certain clusters like Cluster 1 reaching their peak at approximately 0.32 around 50 nanoseconds, while Cluster 14 only reaching 0.04 at 400 nanoseconds. The difference in multipath characteristics between the industrial environment's dense clustering and the outdoor setting's spread-out clusters is highlighted.

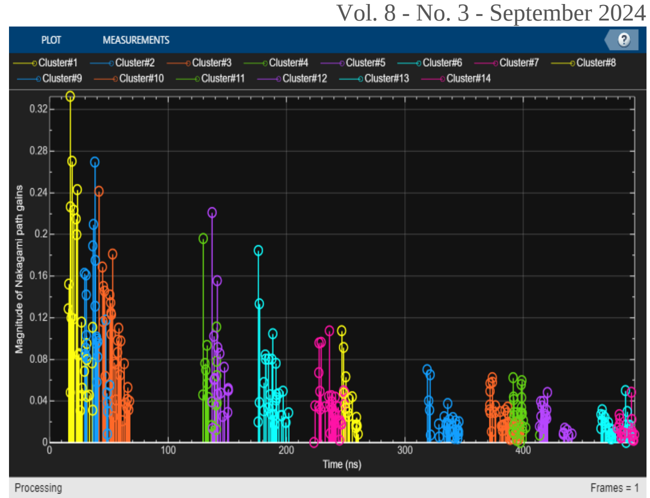

Fig. 16 Comparison of Nakagami path gains in industrial and outdoor environments.

In summary, the performance analysis of UWB channel models, facilitated through simulation and visualization, underscores the necessity for environment-specific adjustments in the design and implementation of UWB positioning systems, particularly with regard to indoor environments where safety applications are paramount. The diversity of conditions inherent across various settings renders a universal approach inadequate. Accordingly, future research and system development endeavors must prioritize the development of customized algorithms. These algorithms should efficiently utilize comprehensive channel state information to not only improve the accuracy but also ensure the reliability of UWB positioning systems in environments where precision is critical to safety and operational efficacy.

VI. Conclusion

This paper culminates in the development and implementation of a novel UWB vibrotactile safety monitoring system designed to enhance industrial labor safety and productivity. By integrating vibrating vests with advanced UWB positioning technology, this system offers a proactive approach to monitoring workers' proximity to hazardous zones, ensuring timely alerts are delivered to mitigate potential safety hazards. The block diagram of the system is elaborately structured and executed within a control room setting, allowing for a comprehensive understanding and application of its components. Through an extensive evaluation of the UWB positioning's performance, particularly focusing on the multipath effects prevalent in industrial environments, this research highlights the system's capability to achieve noteworthy placement accuracy under both static and dynamic conditions. Consequently, the findings underscore the significant potential of the proposed UWB vibrotactile safety monitoring system in reducing workplace accidents and fatalities, marking a pivotal step forward in the pursuit of safer industrial workspaces.

References

[1] A. O'Neill, "Share of economic sectors in the global gross domestic product (GDP) from 2012 to 2022," Statista, URL: https://www.statista.com/statistics/256563/share-of-economic-sectors-in-the-global-gross-domestic-product/#:~:text=This%20statistic%20shows%20the%20share,the%20global%20gross%20domestic%20product. (accessed Mar. 29, 2024).

[2] "Employment in industry (% of total employment) (modeled ILO estimate)," World Bank Open Data, URL: https://data.worldbank.org/indicator/SL.IND.EMPL.ZS?end=2022&start=2022&view=chart (accessed Mar. 30, 2024).

[3] "World Statistic," Jul. 13, 2011. URL: https://www.ilo.org/moscow/areas-of-work/occupational-safety-and-health/WCMS_249278/lang--en/index.htm (accessed Mar. 30, 2024).

[4] "Occupational Safety and Health | UN Global Compact." URL: https://unglobalcompact.org/take-action/safety-andhealth (accessed Mar. 30, 2024).

[5] S. Thiede, B. P. Sullivan, R. Damgrave, and E. Lutters, "Real-time locating systems (RTLS) in future factories: technology review, morphology and application potentials," *Procedia CIRP*, vol. 104, pp. 671–676, Jan. 2021, doi: 10.1016/j.procir.2021.11.113.

[6] S. A. Aldossari, "Predicting path loss of an indoor environment using artificial intelligence in the 28-GHz band," *Electronics*, vol. 12, no. 3, p. 497, Jan. 2023, doi: 10.3390/electronics12030497.

[7] L. Barbieri, M. Brambilla, A. Trabattoni, S. Mervic and M. Nicoli, "UWB Localization in a Smart Factory: Augmentation Methods and Experimental Assessment," in *IEEE Transactions on Instrumentation and Measurement*, vol. 70, pp. 1-18, 2021, Art no. 2508218, doi: 10.1109/TIM.2021.3074403.

[8] Y. Salih-Alj, C. Despins and S. Affes, "Design Considerations for an UWB Computationally-Efficient Fast Acquisition System for Indoor Line-of-Sight Ranging Applications," in *IEEE Transactions on Wireless Communications*, vol. 10, no. 8, pp. 2776-2784, August 2011, doi: 10.1109/TWC.2011.060811.102158.

[9] M. Tang, B. Zhou, X. Zhong, X. Liu, and Q. Li, "Enhanced indoor positioning through human-robot collaboration," *Urban Informatics*, vol. 3, no. 1, Feb. 2024, doi: 10.1007/s44212-024-00037-9.

[10] S. Sakhakarmi, "Embedded safety communication system for robust hazard perception of individuals in work zones," Policy Commons, https://policycommons.net/artifacts/1563144/embedded-safety-communication-system-for-robust-hazard-perception-of-individuals-in-work-zones/2252937/ (accessed Mar. 30, 2024).

[11] X. Yang and N. Roofigari-Esfahan, "Vibrotactile alerting to prevent accidents in highway construction work zones: an exploratory study," *Sensors*, vol. 23, no. 12, p. 5651, Jun. 2023, doi: 10.3390/s23125651.

[12] M. Srikulwong and E. O'Neill, "A direct experimental comparison of back array and waist-belt tactile interfaces for indicating direction," *The University of Bath's Research Portal*, 2010. https://researchportal.bath.ac.uk/en/publications/a-direct-experimental-comparison-of-back-array-and-waist-belt-tac

[13] N. Yadav, N. Sadeghi, and J. Kang, "On-Body Placement of Wearable Safety Promotion Devices based on Wireless Communication for Construction Workers-on-Foot: State-of-the-Art Review," *Sensors*, vol. 22, no. 9, p. 3134, Apr. 2022, doi: 10.3390/s22093134.

[14] A. Morrison, H. Knoche, and C. Manresa-Yee, "Designing a vibrotactile language for a wearable vest," in *Lecture Notes in Computer Science*, 2015, pp. 655–666. doi: 10.1007/978-3-319-20898-5_62.

[15] E. Marks and J. Teizer, "Method for testing proximity detection and alert technology for safe construction equipment operation," *Construction Management and Economics*, vol. 31, no. 6, pp. 636–646, Jun. 2013, doi: 10.1080/01446193.2013.783705.

[16] R. L. Boring, T. A. Ulrich, and T. Mortenson, "Level-of-Automation Considerations for Advanced Reactor Control Rooms," *in Proceedings of the 11th Nuclear Plant Instrumentation, Control and Human-Machine Interface Technologies*, pp. 1210–1221, Orlando, Feb. 2019.

[17] F. Chen, E. H. C. Choi, N. Ruiz, Y. Shi, and R. Taib, "User interface design and evaluation for control room," *in Proceedings of the 17th Australia Conference on Computer-Human Interaction: Citizens Online: Considerations for Today and the Future*, pp. 1–4, Canberra, Nov. 2005.

[18] S. Sellak, O. Haberchad, S. Ibenyahia and Y. Salih-Alj, "Safety Management System for Factory Workers using UWB Indoor Positioning and Wearable Vibrotactile Guidance: Morocco Case Study," 2023 IEEE International Conference on Mechatronics and Automation (ICMA), Harbin, Heilongjiang, China, 2023, pp. 1509-1514, doi: 10.1109/ICMA57826.2023.10215963.

[19] S. Sellak, O. Haberchad, S. Ibenyahia and Y. Salih-Alj, "A UWB Vibrotactile Safety Monitoring System for Factory Environments," 2023 7th IEEE Congress on Information Science and Technology (CiSt), Agadir - Essaouira, Morocco, 2023, pp. 305-310, doi: 10.1109/CiSt56084.2023.10409869.

[20] Accueil, URL : https://industrial-estate.gov.ma/?lang=en (accessed Mar. 30, 2024).

[21] B. Lembrikov, Ed., Ultra Wideband. Sciyo, 2010. doi: 10.5772/276.

[22] C. Cho and J. Park, "An Embedded Sensory System for worker Safety: prototype development and evaluation," *Sensors*, vol. 18, no. 4, p. 1200, Apr. 2018, doi: 10.3390/s18041200.

[23] J. Müller, T. Schwarz, S. Butscher, and H. Reiterer, "Back to tangibility: a post-WIMP perspective on control room design," *Proceedings of the 2014 International Working Conference on Advanced Visual Interfaces*, May 2014. doi:10.1145/2598153.2598161

[24] C. Sandom and R. S. Harvey, "Control room design," in *Human factors for engineers*, London: Institution of Engineering and Technology - IET, 2009, pp. 203–233

[25] Kl Y. Wu, H. Ni, C. Mao, J. Han, and W. Xu, "Non-intrusive human vital sign detection using MMWAve Sensing Technologies: A review," *ACM Transactions on Sensor Networks*, vol. 20, no. 1, pp. 1–36, Nov. 2023, doi: 10.1145/3627161.

[26] M. Srikulwong, and E. O'Neill, "A Direct Experimental Comparison of Back Array and Waist-Belt Tactile Interfaces for Indicating Direction," Paper presented at Workshop on Multimodal location-based techniques for extreme navigation, Pervasive 2010.

[27] S. Sakhakarmi, J. W. Park, and A. Singh, "Tactile-based wearable system for improved hazard perception of worker and equipment collision," Automation in Construction, vol. 125, p. 103-613, May. 2021

[28] M. Delamare, R. Boutteau, X. Savatier, and N. Iriart, "Static and dynamic evaluation of an UWB localization system for industrial applications," *Sci*, vol. 2, no. 2, p. 23, Apr. 2020, doi: 10.3390/sci2020023.

[29] "UWB Channel Models," MATLAB & Simulink, MathWorks China. [Accessed on 15-Feb-2024]. Available: https://ww2.mathworks.cn/help/comm/ug/uwb-channel-model.html

AUTHORS BIOGRAPHIES

Sofya Sellak is a general engineering student with a thematic area in Artificial Intelligence at Akhawayn University in Ifrane (AUI). She spent one year study abroad in both Technical University of Ostrava in Czech Republic and University of Malaya in Malaysia. She was a former member of AUI Mechatronics Club where she participated in various international robotics competitions. She has published two papers. She is currently working part-time as a scientific consultant at Leyton. Her research interests include robotics, mechatronics, and computer vision.

Oumayma Haberchad is a General Engineering student with a concentration in Mechatronics at Al Akhawayn University in Ifrane (AUI). She served as a data analyst at the office of institutional research and effectiveness. She participated in fieldwork experiments to collect data on risk-taking in rural areas. She has published three papers. Her research interests include sustainable manufacturing, robotization, digitalization, data analysis, and geographic information systems.

Yassine Salih Alj received the Bachelor's degree in microelectronics from the University of Quebec at Montreal (UQAM), Montreal, Quebec, Canada, in 2001, and the Master's degree in electrical engineering from the École de Technologie Supérieure (ETS), Montreal, Quebec, Canada, in 2003, and the Ph.D. degree in Telecommunications from the National Institute of Scientific Research – Energy, Materials & Telecommunications (INRS-Telecom), Montreal, Quebec, Canada, in 2008. He served as a research assistant at the Telebec Underground Communications Research Laboratory (LRTCS) from 2005 to 2008, and then during 2009 as a Postdoctoral Fellow at Poly-Grames Research Center, of the École Polytechnique de Montréal, Montreal, Quebec, Canada. He is currently working as a permanent faculty member at the School of Science and Engineering (SSE) of Al Akhawayn University in Ifrane (AUI), Morocco, where he also served during 2019-2022 as Academic Coordinator for General Engineering programs. He has published over 70 publications and has been actively involved in IEEE events for the past five years, where he chaired and served as Technical Program Member or as distinguished reviewer for over 100 conferences. His research interests are in the areas of Wireless Communications, Indoor Positioning, UWB (Ultra-Wideband), Smart Systems, GPS (Global Positioning System) and Engineering Education.